APS physics

CHORUS

This is the accepted manuscript made available via CHORUS. The article has been published as:

Ion Correlation Effects in Salt-Doped Block Copolymers

Jonathan R. Brown, Youngmi Seo, and Lisa M. Hall

Phys. Rev. Lett. **120**, 127801 — Published 22 March 2018

DOI: 10.1103/PhysRevLett.120.127801

Ion Correlation Effects in Salt-Doped Block Copolymers

Jonathan R. Brown,* Youngmi Seo, and Lisa M. Hall*

William G. Lowrie Department of Chemical and Biomolecular Engineering, The Ohio State University, 151 W. Woodruff Ave., Columbus, OH 43210

E-mail: brown.4972@osu.edu; hall.1004@osu.edu

Abstract

We apply classical density functional theory to study how salt changes the microphase morphology of diblock copolymers. Polymers are freely jointed and one monomer type favorably interacts with ions, to account for the selective solvation that arises from different dielectric constants of the microphases. By including correlations from liquid state theory of an unbound reference fluid, the theory can treat chain behavior, microphase separation, ion correlations, and preferential solvation, at same coarse grained level. We show good agreement with molecular dynamics simulations.

Salt-doped microphase separated copolymers have potential as mechanically robust battery electrolytes[1–14] and in other ion transport applications.[15–20] One block (e.g. polyethylene oxide, PEO) is soft and conducts lithium ions; the other block (e.g. polystyrene, PS) can provide mechanical strength to prevent growth of lithium dendrites between electrodes.[21–23] Related ionic liquid containing block copolymers are used as chemical actuators; ions move in response to an applied electric field, causing the material to bend.[24–26] Salt may also be added to copolymers to tune the degree of phase segregation or change microphase morphology (without changing temperature or polymer chemistry), which is of both practical and scientific interest.[16,27–31]

Neat AB diblock copolymers microphase separate into various ordered structures; morphology depends primarily on composition (quantified by f_A, the fraction of "A" monomers), and segregation strength χN, where χ is the Flory parameter which quantifies chemical incompatibility of the two components and N is the degree of polymerization.[32,33] Salt dissolves predominantly in one microphase, primarily due to the different dielectric constants (less energy is required to place an ion in a medium of higher dielectric constant, as described by the ion's Born energy).[34] Due to the additional favorable interactions with one phase, salt enhances segregation between polymer blocks: a disordered system can be ordered by adding salt, and as more salt is added, the domain spacing of the resulting microstructure increases.[29,30] The distribution of ions is of interest as it is thought to impact transport properties. For PS-PEO-like materials with Li^+ salts, some experimental work suggests the salt is concentrated in the middle of the PEO-like domain[3] while other work shows a uniform distribution throughout that domain.[35] Local chemical interactions are also relevant; in polymer battery electrolytes, both strong complexation of Li^+ with ether oxygens along the chain and the extent to which Li^+ pairs or interacts with anions are crucial determinants of ion transport.[36–38]

While microphase separating copolymers have been treated at the mean field level with great success, salt-doped systems contain ions with strong correlations and long-ranged interactions, making their behavior challenging to capture using the same methods. Among the body of theoretical and simulation work on salt-containing copolymers,[34,39–48] recent work from Wang and coworkers using self-consistent field theory (SCFT) is particularly relevant here, as their model included several features meant to mimic lithium salt-doped PS-PEO.[34,39–41] Specifically, because the two blocks have different dielectric constants, a Born solvation energy term was used to drive the ions to increase the segregation between the blocks. Li^+ complexation was modeled by forcing cations to reversibly bond to the PEO-like chain. They argue that since the anions do not get close enough to form strong ion pairs, Coulombic correlations can be neglected, and the Born solvation term drives phase behavior.

This model captured important experimental trends, including increasing effective χ with the addition of salt and a phase diagram showing coexistence between a higher salt content, microphase separated structure and a lower salt content, disordered phase. Olvera de la Cruz and coworkers also used SCFT for related block copolymer and blend systems.[42–44] While the polymers are treated as (infinitely thin) Gaussian chains, their calculations include ion correlations from liquid state theory of a restricted primitive model (in which the ions have a hard core). In their SCFT model, ion concentration is proportional to PEO-type monomer concentration (motivated by considering that cations are bound to the solvating chains and the system is locally electrically neutral). They find that the addition of strong ion correlations can greatly alter the phase diagram.

Meanwhile, Qin and de Pablo simulated coarse grained PS-PEO with salt, including explicit Coulombic interactions.[45] They neglect Born energy but set a negative χ between cations and the PEO-like block to model Li^+-EO complexation. They find that at high Bjerrum length, adding small amounts of salt orders the material. However, for this model at large ion concentrations, the fact that the salt acts as a diluent becomes important enough that further salt addition disorders the material again. More chemically detailed simulations have also been performed; in particular, Ganesan and coworkers performed atomistic simulations of PS-PEO + $LiPF_6$, with a multi-scale approach used for better equilibration.[47] They also find that a small amount of salt increases the tendency to order (i.e. increases domain spacing) but that the domain spacing decreases with concentration at high salt concentrations; they note a similar effect was seen experimentally in Polycaprolactone-b-PEO + $LiClO_4$.[49]

In both of these simulation studies, a significant amount of ions existed in the PS-like phase, while in the current work, we consider strong preferential solvation. Additionally, if ions act as a diluent, one would expect that diffusion would increase with ion concentration, but in fact, the opposite is observed.[50,51] In our simulations, strong ion-polymer interactions are necessary to match the trend of diffusion decreasing with increased ion concentration.[52]

We introduce a different theoretical approach, classical fluids density functional theory (fDFT), to treat monomer and ion packing and correlations on the same level, and compare with molecular dynamics (MD) simulations. This approach takes advantage of well-studied existing functionals describing hard core monomer-scale packing and bonding of chains. We add ion correlations obtained from liquid state theory calculations of ions and solvent; correlations are added to the fDFT after subtracting the hard core portion (as these are included in the existing fDFT framework). Note that the liquid state theory portion of work of the Olvera de la Cruz group used their Debye-Hückel extended mean spherical approximation (DHEMSA) closure[53] to consider ions in a continuous dielectric medium and includes the hard core effects, leading to a qualitatively different behavior in free energy as a function of ion content.[52] Also, it is possible to precisely calculate the interactions between charged spheres in a dielectric continuum (including polarization effects), given that the spheres have an inner continuum dielectric constant that is different from that of the medium.[54–56] However, here we aim to describe the most important features of the system using only simple pairwise potentials.

In both fDFT and MD, we consider a system of freely jointed, AB diblock chains with ions of equal and opposite charge. All coarse grained beads are the same size ($\sigma = 1$). In mapping to experimental systems, the relevant length scale to preserve is the contact distance between ions, thus, the ions here can be thought to represent an "average" of the anion and cation. In the case of the Li^+ and much larger anions such as bis(trifluoromethane)sulfonimide (TFSI) dissolved in PEO, the average of the ion diameters is similar to the length over which the PEO chain is approximately fully flexible (the size of our monomer beads), and we note that with a more detailed mapping one might also use a slightly larger ion size to account for some proportion of the ether oxygens tightly complexed with the Li^+. (Due to this complexation, the distance from Li^+ to the center of a $TFSI^-$ anion in PEO has been found to be around 0.65nm,[37] and the diameter of $TFSI^-$ is $\approx$ 0.7nm.[57] These lengths are similar to the Kuhn length of PEO, reported between 0.8 and 1.1 nm.)[58,59] Because ions are identical here (except

as discussed in the Supplemental Material), their density profiles are identical and there is naturally no overall charge separation. This is representative of the systems we wish to consider, as recent experimental work[35] and simulations that consider significant asymmetry between cation and anion interactions both show negligible charge separation.[45,47,52]

In fDFT,[60–62] excluded volume and chain connectivity are modeled with the White Bear hard sphere functional[63–65] and iSAFT functional,[66] respectively. For MD,[67,68] we employ the standard Kremer-Grest model.[69,70] Blocks are driven to microphase separate by a larger repulsion between unlike beads. To model preferential solvation of ions into the PEO-like phase, we introduce a potential between ions and A beads, $u_{A\pm}(r) = -S_{A\pm}(1/r)^4$, and between ions and other ions, $u_{\pm\pm}(r) = -S_{\pm\pm}(1/r)^4$. We aim to represent the degree to which ions interact with the higher dielectric constant medium, which can be considered to contain local dipoles that can reorient within a coarse-grained bead (not explicitly represented here), and this is the same form as an ion-induced dipole interaction.

The $1/r^4$ form can also be derived explicitly from the interaction between an ion and a polarizable coarse-grained bead using a classical Drude-type model for polarizability.[71] Additionally, to first approximation, the average internal energy per particle from solvation is proportional to $1/\sigma$ (calculated from the integral of the potential over all space outside of the hard core), which is the same scaling with ion size as the Born energy,[34,72] and a similar form can be found calculating the energy of the electric field due to a charge in a dielectric medium.[73] However, the $1/r^4$ is not necessarily the simplest possible model that produces the trends we find herein. A recent study showed that some properties of ions in water can be reproduced in an even simpler coarse-grained model that uses the LJ potential form for all interactions with adjusted interactions to describe ion solvation; specifically, the interaction strength was adjusted by an amount proportional to the Born energy, and the diffusion constants of such ions followed similar trend as in experiments.[74] To give a sense of the sensitivity of the results on the potential form, we report in the Supplemental Material fDFT results using the simplest attractive potential form, a square well. We also consider

other small changes, including using polymeric liquid state theory.[75] The basic features of selective solvation (e.g., selective ion addition leading to an increase in effective segregation) are reproduced, but the sharp change in the square well potential means that the ion density profile shows effects of layering near the interface that does not occur with the smoother $1/r^4$ potential.

The solvation potential should be considered phenomenological, especially regarding its strength, which we vary widely to observe the possible behaviors of such a model. The ion-ion solvation term can be nonzero to model the polar, bulky anions often used with Li^+ or both polar ions of an ionic liquid. Ions also experience Coulombic interactions ($u_{ij}^{\mathrm{Coul}}(r) = z_i z_j l_B / r$, where z_i is charge number and l_B is nondimensionalized Bjerrum length). Implementation of these additional terms is straightforward in MD, using a reciprocal-space method for the long range Coulombic interactions. In fDFT, effects of ion correlations due to Coulombic interactions and solvation are derived from liquid state theory. The liquid state theory considers a reference fluid of the A phase (consisting only of unbonded A beads and salt), as the salt is expected to exist primarily in the A microphase. We apply these potentials with the hypernetted-chain (HNC) closure to solve the Ornstein-Zernike equation;[76,77] the difference between the direct correlation functions of the system with these potentials and with only hard spheres is used to approximate the correlations within fDFT. While in principle this function would vary with location in the box, in this approximation it is fixed to its value in the bulk A phase.[63] Since both ionic species are identical, Poisson's equation is trivially satisfied.

For context in mapping to experimental materials, we first consider PEO at $T = 400$K (at which temperature the polymer is non-crystalline), which has a dielectric constant of $\kappa_{\mathrm{PEO}} \approx 7.5$,[34,78,79] as the ion solvating (conducting) phase. If the coarse grained beads have diameter $\sigma = 0.7$nm, then the Bjerrum length $l_B = e^2/4\pi\epsilon_0\kappa k_B T$ in the PEO phase is $l_B \approx 8.0\sigma$. Of course, the actual experimental system has significant local variation in dielectric properties; the dielectric constant of PS has been reported in the literature as

$\kappa_{\mathrm{PS}} = 2.5$.[80,81] Thus, if ions were to exist within the PS phase, they should experience a much stronger Coulomb interaction. Here, we focus on materials with strong preferential solvation, such that the vast majority of ion-ion interactions occur well within the conducting phase, thus, we expect the ion interaction strength in the other phase is not a crucial determinant of overall material's behavior.[30] We expect this model will perform better in cases where there are fewer ions very close to the interface, where the dielectric properties change quickly. Because the solvation potential is motivated by ion-dipole interactions, one may expect that l_B and $S_{A\pm}$ must depend on each other for consistency between ion interactions and solvation interactions with respect to the ion charge and length scale. However, because we consider no solvation interaction with B ($S_{B\pm} = 0$), $S_{A\pm}$ should be understood to represent the increased preferential solvation in A versus B, rather than the absolute energy of solvation (Born energy). Thus, $S_{A\pm}$ and l_B are partially independent in that we consider l_B to be tied to the dielectric constant of the conducting phase but $S_{A\pm}$ to depend on the difference in dielectric constants of the two microphases. The difference between the Born energy $V_{\mathrm{Born}} = l_B k_B T/\sigma$ in PS-PEO with local dielectric constants of 7.5 and 2.5 is about $16 k_B T$.[34,72] Alternatively, if the nonsolvating block is polycaprolactone (PCL),[49] with dielectric constant of 4.4,[82] then the Born energy difference is $5.6 k_B T$. Using a coarse approximation for the pair distribution function (neglecting correlations), $g(r) \approx \exp(-u(r))$, to estimate the solvation energy per ion $V = \rho \int g(r) u(r) \mathrm{d}\boldsymbol{r}$, this would correspond to $S_{A\pm} \approx 1.1$ for PS-PEO and 0.47 for PCL-PEO.

Very different combinations of these parameters may be relevant to different experimental systems depending on temperature, bead size, and polymer choice. Here we consider a range of possible values to show the independent and collective effects of each of the major ion interaction parameters on the system; specifically, we consider $l_B = 5$ and 10σ, as well as $l_B = 0$ for reference, and $S_{A\pm} = 0.3$, 0.5, 0.6, and 1.0.

Density profiles showing the effect of the two ionic energy parameters at low ion concentration are shown in Figure 1. We do not expect quantitative agreement due to differences in

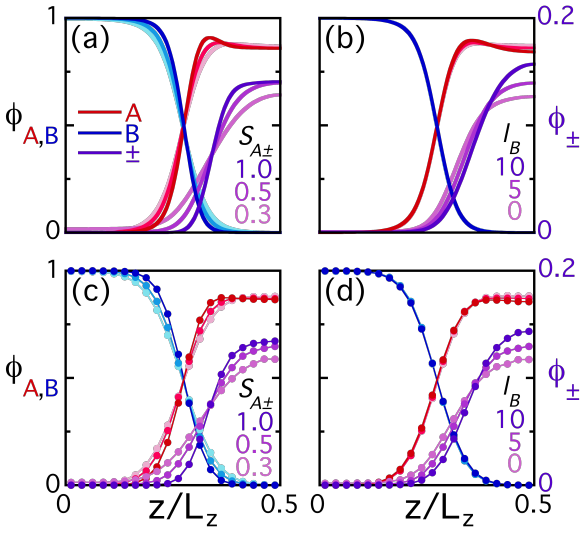

Figure 1: Density order parameter ($\phi_\alpha(z) = \rho_\alpha(z)/\rho_{\text{tot}}(z)$) of polymers (red A beads, blue B beads, left axes) and ions (purple, right axes) plotted vs. distance across the lamellae from fDFT (a,b) and MD (c,d). (a,c) $l_B = 5$ and $S_{A\pm}$ is as labeled. (b,d) $S_{A\pm} = 0.5$ and l_B is as labeled. $\epsilon_{AB} - \epsilon_{AA} = 1$, $S_{\pm\pm} = 0$, $N_A = 26$, $N_B = 34$, and $[+]/[A] = 0.056$. At this relatively small ion concentration, $S_{\pm\pm}$ does not have a noticeable effect on the density profiles.

the models: our MD model has softer repulsive interactions, a shorter average bond length, and a different ϵ_{AB} to χ_{AB} mapping because the fDFT A-B interactions are at the mean field level (and do not include fluctuations).[62] However, fDFT and MD results agree qualitatively, suggesting that the reference fluid method used to obtain correlations captures the important effects of ions in this region of the parameter space. As Coulombic interactions are strengthened (i.e. as l_B is increased), the salt concentrates in the middle of the A lamellae, whereas, as the solvation term ($S_{A\pm}$) is increased, the salt is more equally distributed in the A phase. Thus, there is a competition between Coulombic interactions and preferential solvation of ions in determining the location of ions within the lamellae. Experimental work found that the ions being well segregated from the B phase promotes higher ion conductivity,[3,18] so understanding the balance between Coulombic and preferential solvation energies and how this impacts concentration profiles may aid in designing more conductive materials. Neat polymer mobility is another crucial factor; for example, using tapered sequences (adding a gradient block between the pure A and B blocks) inherently leads to broader interfaces, with

effects on the ion concentration profile that are not fully understood. However, tapering can lead to increased conductivity likely because it decreases the glass transition temperature (increases segmental mobility).[10]

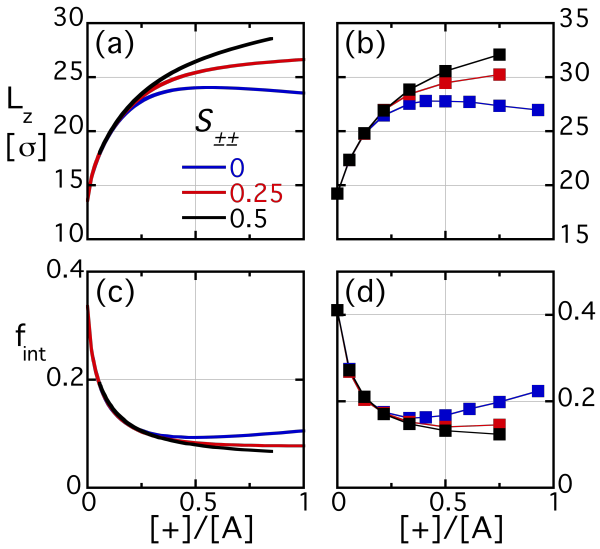

Figure 2: Domain spacing (a,b) and fraction of interface (c,d) plotted vs. the ratio of cations to A beads from fDFT (a,c) and MD (b,d). $\epsilon_{AB} - \epsilon_{AA} = 1$, $S_{A\pm} = 0.5$, and $l_B = 10$. $S_{\pm\pm} = 0.5$, 0.25, and 0, as labeled. Different values of $S_{A\pm}$ and l_B show similar trends.

Lamellar domain spacing and interfacial fraction (f_{int}) are shown in Figure 2 as a function of salt content. As salt is added, the preferential solvation effect causes the system to phase segregate more strongly, increasing domain spacing and reducing interfacial width. Without the additional solvation between ions, however, the trend in domain spacing is nonmonotonic, decreasing at high salt concentrations, as was seen in previous theoretical work.[44] This nonmonotonic behavior was not observed experimentally in PS-PEO systems,[2,29,30] where adding salt always increases domain spacing. However, in a study of PCL-PEO with $LiClO_4$, the domain spacing at high salt concentrations did decrease,[49] likely due to the weaker dielectric inhomogeneity between the PCL and PEO domains causing more ions to dissolve in the PCL domain, inducing a dilution effect.[47] In some studies, the interfacial width is used as a measure of effective χ (as there is a one-to-one relationship between χ and f_{int} for neat diblock copolymers); in this sense, effective χ increases rapidly at low salt concentrations, but

decreases or plateaus at high salt concentrations, depending on $S_{\pm\pm}$. Many have reported a linear relationship between effective χ and salt concentration,[4,27,30] but this seems to only apply at low salt concentrations. A plateau in effective χ with salt concentration has been observed experimentally in PS-PEO.[29]

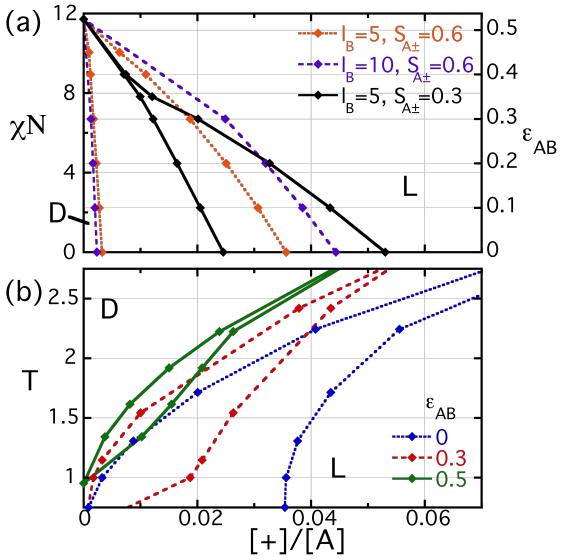

Figure 3: Phase diagrams of salt doped block copolymers, where D indicates the disordered phase, L indicates lamellae, and a gap between these regions indicates phase coexistence. a) Phase diagrams where the block copolymer segregation strength (χN) is plotted vs. ion fraction ($[+]/[A]$) for l_B and $S_{A\pm}$, as labelled. b) Phase diagrams where the energy parameters (ϵ_{AB}, l_B, and S) are all scaled by temperature T. The three curves have $l_B = 5$ and $S_{A\pm} = 0.6$ (the orange system in (a)) with ϵ_{AB} as labeled. $S_{\pm\pm} = S_{A\pm}/2$, however, the results are insensitive to the choice of $S_{\pm\pm}$ at these concentrations.

Figure 3 shows fDFT phase diagrams as a function of salt concentration at different values of l_B, $S_{A\pm}$, ϵ_{AB}, and temperature (T). A two phase region develops between the disordered and lamellar phases, as was seen in experiment,[28,29] and in previous theory that included the effect of ion solvation.[40] The width of the coexistence region is narrow when the solvation energy term is weak (at high temperature or low $S_{A\pm}$) or when the neat polymer is nearly or already microphase separated (at low temperature or high χN). The two phase region of the weak ionic interaction system (black) is small but nonzero for all χN considered. We do not consider the hexagonally packed cylinder phase here, which may be the preferred phase

for systems at high χN in Figure 3a, due to asymmetry at low ion content.[31,83,84] Increasing either $S_{A\pm}$ or l_B widens the coexistence region; the effect of solvation appears to be larger.

Our method accounts for both ion correlations (using liquid state theory) and Born energy (using a phenomenological $1/r^4$ potential) in salt-doped block copolymers. Applying the solvation potential between ions themselves is necessary to replicate the experimental trend in domain spacing. We validate our model by comparing to MD simulations, showing that fDFT and MD results qualitatively agree; differences in the models (such as the different bond lengths and the use of hard spheres in fDFT) prevent the comparison from being quantitative. In a future publication we will use these MD simulations to study dynamical behavior. Finally, we reproduce experimental and previous theoretical results that these systems form a coexistence region near the ODT under the right conditions. Further studies are ongoing, including mapping a full phase diagram and explicitly including the complexation of ions to the chain via breakable bonds.

Acknowledgement

We thank Thomas Epps, III, Zhen-Gang Wang, Issei Nakamura, and Amalie Frischknecht for useful discussions. This material is based upon work supported by the U.S. Department of Energy, Office of Science, Office of Basic Energy Sciences, under Award Number DE-SC0014209 (JRB and LMH). Regarding MD simulations of Y.S., this material is based upon work supported by the National Science Foundation under Grant No. 1454343. We thank the Ohio Supercomputer Center for computing time.

References

(1) Hallinan, D. T.; Balsara, N. P. Polymer Electrolytes. *Annual Review of Materials Research* **2013**, *43*, 503–525.

(2) Panday, A.; Mullin, S.; Gomez, E. D.; Wanakule, N.; Chen, V. L.; Hexemer, A.; Pople, J.; Balsara, N. P. Effect of Molecular Weight and Salt Concentration on Conductivity of Block Copolymer Electrolytes. *Macromolecules* **2009**, *42*, 4632–4637.

(3) Gomez, E. D.; Panday, A.; Feng, E. H.; Chen, V.; Stone, G. M.; Minor, A. M.; Kisielowski, C.; Downing, K. H.; Borodin, O.; Smith, G. D.; Balsara, N. P. Effect of Ion Distribution on Conductivity of Block Copolymer Electrolytes. *Nano Letters* **2009**, *9*, 1212–1216.

(4) Wanakule, N. S.; Panday, A.; Mullin, S. A.; Gann, E.; Hexemer, A.; Balsara, N. P. Ionic Conductivity of Block Copolymer Electrolytes in the Vicinity of OrderDisorder and OrderOrder Transitions. *Macromolecules* **2009**, *42*, 5642–5651.

(5) Chintapalli, M.; Le, T. N. P.; Venkatesan, N. R.; Mackay, N. G.; Rojas, A. A.; Thelen, J. L.; Chen, X. C.; Devaux, D.; Balsara, N. P. Structure and Ionic Conductivity of Polystyrene-block-poly(ethylene oxide) Electrolytes in the High Salt Concentration Limit. *Macromolecules* **2016**, *49*, 1770–1780.

(6) Miller, T. F.; Wang, Z.-G.; Coates, G. W.; Balsara, N. P. Designing Polymer Electrolytes for Safe and High Capacity Rechargeable Lithium Batteries. *Accounts of Chemical Research* **2017**, *50*, 590–593.

(7) Young, W.-S.; Epps, T. H. Ionic Conductivities of Block Copolymer Electrolytes with Various Conducting Pathways: Sample Preparation and Processing Considerations. *Macromolecules* **2012**, *45*, 4689–4697.

(8) Young, W.-S.; Kuan, W.-F.; Epps, T. H. Block copolymer electrolytes for rechargeable lithium batteries. *Journal of Polymer Science Part B: Polymer Physics* **2014**, *52*, 1–16.

(9) Gilbert, J. B.; Luo, M.; Shelton, C. K.; Rubner, M. F.; Cohen, R. E.; Epps, T. H. Determination of Lithium-Ion Distributions in Nanostructured Block Polymer Electrolyte

Thin Films by X-ray Photoelectron Spectroscopy Depth Profiling. *ACS Nano* **2015**, *9*, 512–520.

(10) Kuan, W.-F.; Remy, R.; Mackay, M. E.; Epps, T. H. Controlled ionic conductivity via tapered block polymer electrolytes. *RSC Advances* **2015**, *5*, 12597–12604.

(11) Chandrashekar, S.; Oparaji, O.; Yang, G.; Hallinan, D. Communication7Li MRI Unveils Concentration Dependent Diffusion in Polymer Electrolyte Batteries. *Journal of The Electrochemical Society* **2016**, *163*, A2988–A2990.

(12) Hallinan, D. T.; Rausch, A.; McGill, B. An electrochemical approach to measuring oxidative stability of solid polymer electrolytes for lithium batteries. *Chemical Engineering Science* **2016**, *154*, 34–41.

(13) Morris, M. A.; An, H.; Lutkenhaus, J. L.; Epps, T. H. Harnessing the Power of Plastics: Nanostructured Polymer Systems in Lithium-Ion Batteries. *ACS Energy Letters* **2017**, *2*, 1919–1936.

(14) Morris, M. A.; Gartner, T. E.; Epps, T. H. Tuning Block Polymer Structure, Properties, and Processability for the Design of Efficient Nanostructured Materials Systems. *Macromolecular Chemistry and Physics* **2017**, *218*, 1600513.

(15) Choi, I.; Ahn, H.; Park, M. J. Enhanced Performance in LithiumPolymer Batteries Using Surface-Functionalized Si Nanoparticle Anodes and Self-Assembled Block Copolymer Electrolytes. *Macromolecules* **2011**, *44*, 7327–7334.

(16) Jo, G.; Ahn, H.; Park, M. J. Simple Route for Tuning the Morphology and Conductivity of Polymer Electrolytes: One End Functional Group is Enough. *ACS Macro Letters* **2013**, *2*, 990–995.

(17) Park, M. J.; Kim, S. Y. Ion transport in sulfonated polymers. *Journal of Polymer Science Part B: Polymer Physics* **2013**, *51*, 481–493.

(18) Kim, O.; Jo, G.; Park, Y. J.; Kim, S.; Park, M. J. Ion Transport Properties of Self-Assembled Polymer Electrolytes: The Role of Confinement and Interface. *The Journal of Physical Chemistry Letters* **2013**, *4*, 2111–2117.

(19) Jung, H. Y.; Kim, O.; Park, M. J. Ion Transport in Nanostructured Phosphonated Block Copolymers Containing Ionic Liquids. *Macromolecular Rapid Communications* **2016**, *37*, 1116–1123.

(20) Oparaji, O.; Zuo, X.; Hallinan Jr., D. T. Crystallite dissolution in PEO-based polymers induced by water sorption. *Polymer* **2016**, *100*, 206–218.

(21) Hallinan, D. T.; Mullin, S. A.; Stone, G. M.; Balsara, N. P. Lithium Metal Stability in Batteries with Block Copolymer Electrolytes. *Journal of The Electrochemical Society* **2013**, *160*, A464–A470.

(22) Harry, K. J.; Hallinan, D. T.; Parkinson, D. Y.; MacDowell, A. A.; Balsara, N. P. Detection of subsurface structures underneath dendrites formed on cycled lithium metal electrodes. *Nature Materials* **2014**, *13*, 69–73.

(23) Harry, K. J.; Higa, K.; Srinivasan, V.; Balsara, N. P. Influence of Electrolyte Modulus on the Local Current Density at a Dendrite Tip on a Lithium Metal Electrode. *Journal of The Electrochemical Society* **2016**, *163*, A2216–A2224.

(24) Kim, O.; Shin, T. J.; Park, M. J. Fast low-voltage electroactive actuators using nanostructured polymer electrolytes. *Nature Communications* **2013**, *4*, 2208.

(25) Park, M. J.; Choi, I.; Hong, J.; Kim, O. Polymer electrolytes integrated with ionic liquids for future electrochemical devices. *Journal of Applied Polymer Science* **2013**, *129*, 2363–2376.

(26) Kim, O.; Kim, S. Y.; Park, B.; Hwang, W.; Park, M. J. Factors Affecting Electrome-

chanical Properties of Ionic Polymer Actuators Based on Ionic Liquid-Containing Sulfonated Block Copolymers. *Macromolecules* **2014**, *47*, 4357–4368.

(27) Wanakule, N. S.; Virgili, J. M.; Teran, A. A.; Wang, Z.-G.; Balsara, N. P. Thermodynamic Properties of Block Copolymer Electrolytes Containing Imidazolium and Lithium Salts. *Macromolecules* **2010**, *43*, 8282–8289.

(28) Thelen, J. L.; Teran, A. A.; Wang, X.; Garetz, B. A.; Nakamura, I.; Wang, Z.-G.; Balsara, N. P. Phase Behavior of a Block Copolymer/Salt Mixture through the Order-to-Disorder Transition. *Macromolecules* **2014**, *47*, 2666–2673.

(29) Teran, A. A.; Balsara, N. P. Thermodynamics of Block Copolymers with and without Salt. *The Journal of Physical Chemistry B* **2014**, *118*, 4–17.

(30) Young, W.-S.; Epps, T. H. Salt Doping in PEO-Containing Block Copolymers: Counterion and Concentration Effects. *Macromolecules* **2009**, *42*, 2672–2678.

(31) Kuan, W.-F.; Reed, E. H.; Nguyen, N. A.; Mackay, M. E.; Epps, T. H. Using tapered interfaces to manipulate nanoscale morphologies in ion-doped block polymers. *MRS Communications* **2015**, *FirstView*, 1–6.

(32) Matsen, M. W.; Schick, M. Stable and unstable phases of a diblock copolymer melt. *Physical Review Letters* **1994**, *72*, 2660–2663.

(33) Cochran, E. W.; Garcia-Cervera, C. J.; Fredrickson, G. H. Stability of the Gyroid Phase in Diblock Copolymers at Strong Segregation. *Macromolecules* **2006**, *39*, 2449–2451.

(34) Nakamura, I.; Balsara, N. P.; Wang, Z.-G. Thermodynamics of Ion-Containing Polymer Blends and Block Copolymers. *Physical Review Letters* **2011**, *107*, 198301.

(35) Shelton, C. K.; Dura, J.; Epps, T. H. Quantifying lithium salt distributions in nanostructured ion-conducting polymer domains: a neutron reflectivity study. Bulletin of the American Physical Society. New Orleans, Louisiana, 2017.

(36) Donoso, J. P.; Bonagamba, T. J.; Panepucci, H. C.; Oliveira, L. N.; Gorecki, W.; Berthier, C.; Armand, M. Nuclear magnetic relaxation study of poly(ethylene oxide)lithium salt based electrolytes. *The Journal of Chemical Physics* **1993**, *98*, 10026–10036.

(37) Mao, G.; Saboungi, M.-L.; Price, D. L.; Armand, M. B.; Howells, W. S. Structure of Liquid PEO-LiTFSI Electrolyte. *Physical Review Letters* **2000**, *84*, 5536–5539.

(38) Mao, G.; Saboungi, M.-L.; Price, D. L.; Badyal, Y. S.; Fischer, H. E. Lithium environment in PEO-LiClO4 polymer electrolyte. *EPL (Europhysics Letters)* **2001**, *54*, 347.

(39) Nakamura, I.; Wang, Z.-G. Salt-doped block copolymers: ion distribution, domain spacing and effective parameter. *Soft Matter* **2012**, *8*, 9356–9367.

(40) Nakamura, I.; Balsara, N. P.; Wang, Z.-G. First-Order Disordered-to-Lamellar Phase Transition in Lithium Salt-Doped Block Copolymers. *ACS Macro Letters* **2013**, *2*, 478–481.

(41) Nakamura, I.; Wang, Z.-G. Thermodynamics of Salt-Doped Block Copolymers. *ACS Macro Letters* **2014**, 708–711.

(42) Sing, C. E.; Zwanikken, J. W.; de la Cruz, M. O. Interfacial Behavior in Polyelectrolyte Blends: Hybrid Liquid-State Integral Equation and Self-Consistent Field Theory Study. *Physical Review Letters* **2013**, *111*, 168303.

(43) Sing, C. E.; Zwanikken, J. W.; Olvera de la Cruz, M. Electrostatic control of block copolymer morphology. *Nature Materials* **2014**, *13*, 694–698.

(44) Sing, C. E.; Zwanikken, J. W.; Cruz, M. O. d. l. Theory of melt polyelectrolyte blends and block copolymers: Phase behavior, surface tension, and microphase periodicity. *The Journal of Chemical Physics* **2015**, *142*, 034902.

(45) Qin, J.; de Pablo, J. J. Ordering Transition in Salt-Doped Diblock Copolymers. *Macromolecules* **2016**,

(46) Qin, J.; de Pablo, J. J. Criticality and Connectivity in Macromolecular Charge Complexation. *Macromolecules* **2016**, *49*, 8789–8800.

(47) Sethuraman, V.; Mogurampelly, S.; Ganesan, V. Multiscale Simulations of Lamellar PSPEO Block Copolymers Doped with LiPF6 Ions. *Macromolecules* **2017**, *50*, 4542–4554.

(48) Cao, J.; Riggleman, R. A. Field-theoretic simulations of correlation effects in charged polymers. Bulletin of the American Physical Society. New Orleans, Louisiana, 2017.

(49) Huang, J.; Tong, Z.-Z.; Zhou, B.; Xu, J.-T.; Fan, Z.-Q. Salt-induced microphase separation in poly(ε-caprolactone)-b-poly(ethylene oxide) block copolymer. *Polymer* **2013**, *54*, 3098–3106.

(50) Borodin, O.; Smith, G. D. Mechanism of Ion Transport in Amorphous Poly(ethylene oxide)/LiTFSI from Molecular Dynamics Simulations. *Macromolecules* **2006**, *39*, 1620–1629.

(51) Timachova, K.; Watanabe, H.; Balsara, N. P. Effect of Molecular Weight and Salt Concentration on Ion Transport and the Transference Number in Polymer Electrolytes. *Macromolecules* **2015**, *48*, 7882–7888.

(52) See Supplemental Material.

(53) Zwanikken, J. W.; Jha, P. K.; Cruz, M. O. d. l. A practical integral equation for the structure and thermodynamics of hard sphere Coulomb fluids. *The Journal of Chemical Physics* **2011**, *135*, 064106.

(54) Barros, K.; Luijten, E. Dielectric effects in the self-assembly of binary colloidal aggregates. *Physical review letters* **2014**, *113*, 017801.

(55) Gan, Z.; Wu, H.; Barros, K.; Xu, Z.; Luijten, E. Comparison of efficient techniques for the simulation of dielectric objects in electrolytes. *Journal of Computational Physics* **2015**, *291*, 317–333.

(56) Gustafson, K. S.; Xu, G.; Freed, K. F.; Qin, J. Image method for electrostatic energy of polarizable dipolar spheres. *The Journal of Chemical Physics* **2017**, *147*, 064908.

(57) Largeot, C.; Portet, C.; Chmiola, J.; Taberna, P.-L.; Gogotsi, Y.; Simon, P. Relation between the ion size and pore size for an electric double-layer capacitor. *Journal of the American Chemical Society* **2008**, *130*, 2730–2731.

(58) García Sakai, V.; Maranas, J. K.; Chowdhuri, Z.; Peral, I.; Copley, J. R. D. Miscible blend dynamics and the length scale of local compositions. *Journal of Polymer Science Part B: Polymer Physics* **2005**, *43*, 2914–2923.

(59) Rubinstein, M.; Colby, R. *Polymer Physics*; Oxford University Press, 2003.

(60) Tramonto Software. `https://software.sandia.gov/DFTfluids/index.html`.

(61) Heroux, M.; Salinger, A.; Frink, L. Parallel Segregated Schur Complement Methods for Fluid Density Functional Theories. *SIAM Journal on Scientific Computing* **2007**, *29*, 2059–2077.

(62) Brown, J. R.; Seo, Y.; Maula, T. A. D.; Hall, L. M. Fluids density functional theory and initializing molecular dynamics simulations of block copolymers. *The Journal of Chemical Physics* **2016**, *144*, 124904.

(63) Oleksy, A.; Hansen, J.-P. Towards a microscopic theory of wetting by ionic solutions. I. Surface properties of the semi-primitive model. *Molecular Physics* **2006**, *104*, 2871–2883.

(64) Rosenfeld, Y. Free-energy model for the inhomogeneous hard-sphere fluid mixture and density-functional theory of freezing. *Physical Review Letters* **1989**, *63*, 980–983.

(65) Roth, R. Fundamental measure theory for hard-sphere mixtures: a review. *Journal of Physics: Condensed Matter* **2010**, *22*, 063102.

(66) Jain, S.; Dominik, A.; Chapman, W. G. Modified interfacial statistical associating fluid theory: A perturbation density functional theory for inhomogeneous complex fluids. *The Journal of Chemical Physics* **2007**, *127*, 244904–244904–12.

(67) LAMMPS Molecular Dynamics Simulator. `http://lammps.sandia.gov/`.

(68) Seo, Y.; Brown, J. R.; Hall, L. M. Diffusion of Selective Penetrants in Interfacially Modified Block Copolymers from Molecular Dynamics Simulations. *ACS Macro Letters* **2017**, *6*, 375–380.

(69) Kremer, K.; Grest, G. S. Dynamics of entangled linear polymer melts: A moleculardynamics simulation. *The Journal of Chemical Physics* **1990**, *92*, 5057–5086.

(70) Grest, G. S.; Lacasse, M.-D.; Kremer, K.; Gupta, A. M. Efficient continuum model for simulating polymer blends and copolymers. *The Journal of Chemical Physics* **1996**, *105*, 10583–10594.

(71) Martin, J. M.; Li, W.; Delaney, K. T.; Fredrickson, G. H. Statistical field theory description of inhomogeneous polarizable soft matter. *The Journal of Chemical Physics* **2016**, *145*, 154104.

(72) Wang, Z.-G. Fluctuation in electrolyte solutions: The self energy. *Physical Review E* **2010**, *81*, 021501.

(73) Wang, Z.-G. Effects of Ion Solvation on the Miscibility of Binary Polymer Blends. *The Journal of Physical Chemistry B* **2008**, *112*, 16205–16213.

(74) Andreev, M.; Chremos, A.; de Pablo, J.; Douglas, J. F. Coarse-Grained Model of the Dynamics of Electrolyte Solutions. *The Journal of Physical Chemistry B* **2017**,

(75) Schweizer, K. S.; Curro, J. G. In *Atomistic Modeling of Physical Properties*; Monnerie, P. D. L., Suter, P. D. U. W., Eds.; Advances in Polymer Science 116; Springer Berlin Heidelberg, 1994; pp 319–377.

(76) Hansen, J.-P.; McDonald, I. R. *Theory of Simple Liquids: With Applications to Soft Matter*; Academic Press, 2013.

(77) Hummer, G.; Soumpasis, D. M. Correlations and free energies in restricted primitive model descriptions of electrolytes. *The Journal of Chemical Physics* **1993**, *98*, 581–591.

(78) Porter, C.; Boyd, R. A Dielectric Study of the Effects of Melting on Molecular Relaxation in Poly(ethylene oxide) and Polyoxymethylene. *Macromolecules* **1971**, *4*, 589–594.

(79) Gray, F. M.; Vincent, C. A.; Kent, M. A Study of the dielectric properties of the polymer electrolyte PEO-LiClO4 over a composition range using time domain spectroscopy. *Journal of Polymer Science Part B: Polymer Physics* **1989**, *27*, 2011–2022.

(80) Roberts, S.; Von Hippel, A. A New Method for Measuring Dielectric Constant and Loss in the Range of Centimeter Waves. *Journal of Applied Physics* **1946**, *17*, 610–616.

(81) Yano, O.; Wada, Y. Dynamic mechanical and dielectric relaxations of polystyrene below the glass temperature. *Journal of Polymer Science Part A-2: Polymer Physics* **1971**, *9*, 669–686.

(82) Hegde, V. J.; Gallot-Lavalle, O.; Heux, L. Dielectric study of Polycaprolactone: A biodegradable polymer. 2016 IEEE International Conference on Dielectrics (ICD). 2016; pp 293–296.

(83) Suo, T.; Yan, D.; Yang, S.; Shi, A.-C. A Theoretical Study of Phase Behaviors for Diblock Copolymers in Selective Solvents. *Macromolecules* **2009**, *42*, 6791–6798.

(84) Lai, C.; Russel, W. B.; Register, R. A. Phase Behavior of StyreneIsoprene Diblock Copolymers in Strongly Selective Solvents. *Macromolecules* **2002**, *35*, 841–849.